An introduction to the water recovery x-ray rocket

Drew M. Miles, Randall L. McEntaffer, Ted B. Schultz, Benjamin D. Donovan, James H. Tutt, et al.

Drew M. Miles, Randall L. McEntaffer, Ted B. Schultz, Benjamin D. Donovan, James H. Tutt, Daniel Yastishock, Tyler Steiner, Christopher R. Hillman, Jake A. McCoy, Mitchell Wages, Sam Hull, Abe Falcone, David N. Burrows, Tanmoy Chattopadhyay, Tyler Anderson, Maria McQuaide, "An introduction to the water recovery x-ray rocket," Proc. SPIE 10397, UV, X-Ray, and Gamma-Ray Space Instrumentation for Astronomy XX, 103970R (29 August 2017); doi: 10.1117/12.2274249

SPIE.

Event: SPIE Optical Engineering + Applications, 2017, San Diego, California, United States

An introduction to the water recovery x-ray rocket

Drew M. Miles*[a], Randall L. McEntaffer[a], Ted B. Schultz[a], Benjamin D. Donovan[a], James H. Tutt[a], Daniel Yastishock[a], Tyler Steiner[a], Christopher R. Hillman[a], Jake A. McCoy[a], Mitchell Wages[a], Sam Hull[a], Abe Falcone[a], David N. Burrows[a], Tanmoy Chattopadhyay[a], Tyler Anderson[a], and Maria McQuaide[a]

[a]Pennsylvania State University, Dept. of Astrophysics, 525 Davey Lab, University Park, PA 16802

ABSTRACT

The Water Recovery X-ray Rocket (WRXR) is a sounding rocket payload that will launch from the Kwajalein Atoll in April 2018 and seeks to be the first astrophysics sounding rocket payload to be water recovered by NASA. WRXR's primary instrument is a grating spectrometer that consists of a mechanical collimator, X-ray reflection gratings, grazing-incidence mirrors, and a hybrid CMOS detector. The instrument will obtain a spectrum of the diffuse soft X-ray emission from the northern part of the Vela supernova remnant and is optimized for 3rd and 4th order OVII emission. Utilizing a field of view of $3.25^\circ \times 3.25^\circ$ and resolving power of $\lambda/\delta\lambda$ ≈40-50 in the lines of interest, the WRXR spectrometer aims to achieve the most highly-resolved spectrum of Vela's diffuse soft X-ray emission. This paper presents introductions to the payload and the science target.

Keywords: X-ray, sounding rocket, reflection gratings, hybrid CMOS, Vela, off-plane gratings, instrumentation

1. INTRODUCTION

The Water Recovery X-ray Rocket (WRXR) is a sounding rocket payload that has been designed to fill the gap in X-ray studies between point-source observatories such as Chandra and XMM-Newton and wide-field surveyors, which suffer from poor energy resolution. WRXR's primary instrument is a soft X-ray spectrometer with a $3.25^\circ \times 3.25^\circ$ field of view and resolving power of $\lambda/\delta\lambda$ ≈40-50 in the lines of interest: 3rd and 4th order OVII. The payload is designed to accommodate four independent spectrometer channels but will fly a single channel on this flight due to cost and time constraints. WRXR will serve as a pathfinder for a more complete, multi-channel soft X-ray spectrometer on future flights.

In the WRXR spectrometer, light is collected by a mechanical collimator that has flown successfully on two previous missions[1,2] and sculpts a beam that converges over a 2-meter focal length. Instead of passing through to the focus, light from the collimator is instead intercepted by an array of X-ray gratings that disperses the incident radiation into a component spectrum. Following the grating array is a co-aligned mirror array that reflects light from the ∼100 mm collimator and grating arrays onto a $3.25^\circ \times 3.25^\circ$ mm area at the focal plane, where a hybrid CMOS detector images the spectrum.

Scheduled to launch from the Kwajalein Atoll in April 2018, WRXR seeks to be the first NASA astrophysics payload to launch from a sounding rocket and be recovered from water. Successful water recovery will not only return the instrument for continued development, but will pave the way for future missions to launch recoverable payloads into the ocean and utilize new launch sites. Kwajalein, at a latitude of 9°N, offers a location that is more ideal than currently operated sites (all of which are >30°N)[3] from which to observe the Vela supernova remnant, the science target for the WRXR spectrometer.

*dmiles@psu.edu

UV, X-Ray, and Gamma-Ray Space Instrumentation for Astronomy XX, edited by Oswald H. Siegmund,
Proc. of SPIE Vol. 10397, 103970R · © 2017 SPIE · CCC code: 0277-786X/17/$18 · doi: 10.1117/12.2274249

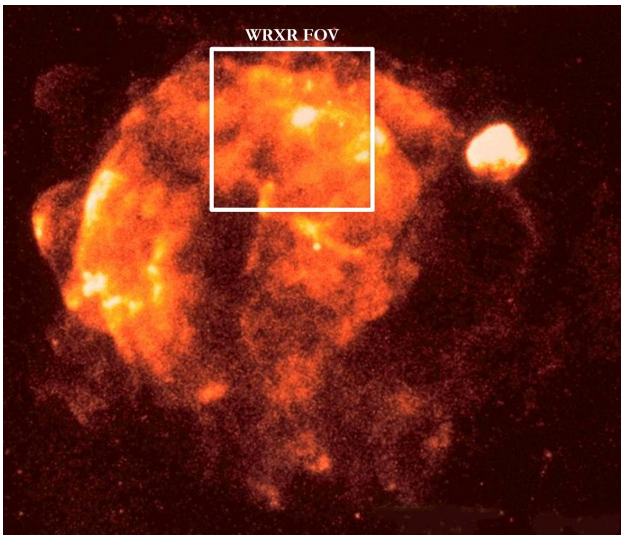

Figure 1. The Vela supernova remnant as seen in the X-ray by the ROSAT satellite. The WRXR field of view will be centered on the bright but relatively unexplored northern part of the remnant.

2. WRXR SCIENCE

WRXR's soft X-ray spectrometer will observe the northern part of the Vela supernova remnant (Fig. 1). This section of the remnant was selected in order to observe a relatively unexplored region of Vela while simultaneously avoiding contamination from the pulsar near the center of the remnant and the two other supernova remnants near the field of view: Puppis A and Vela Jr.

2.1 The Vela supernova remnant

The Vela supernova remnant is shell-type remnant at a distance[4] of ∼250 pc and with an apparent diameter of ∼8°. The morphology of Vela suggests that the local interstellar medium has been swept up by the supernova blast wave or the precursor wind into a nearly spherical zone of interaction. Shock heated plasmas in this zone reach collisional ionization equilibrium on a timescale that is inversely proportional to density; the denser regions therefore equilibrate more quickly and cool more efficiently than rarified regions, which remain hot and have emission at higher energies. This scenario is also seen in other Type II shell remnants[5,6] and a spectrum of the broad emission in the northern part of the remnant will provide a basis for comparison among various shell-type remnants.

Vela's large apparent size, high surface brightness, and low intervening hydrogen column density have made the remnant a common target for both sounding rockets[7,8,9] and space telescopes.[10,11,12,13] However, there is still some disagreement about the prevailing conditions across the remnant; most authors conclude that ionization equilibrium conditions exist (though with different proposed temperature models), but some observations suggest that a second temperature component or non-equilibrium conditions exist to an undetermined extent. Additionally, previous observations suffer from either prohibitively low spectral resolving power (sounding rockets and ROSAT) or a small field of view. WRXR will combine a large FOV and moderate resolving power to perform a new observation on the northern part of the remnant.

2.2 Modeled spectrum

To estimate the spectrum achievable with the WRXR spectrometer, a simulated observation of the Vela supernova remnant was produced. An estimate of the flux from the region of Vela that WRXR will observe was obtained using the HEASARC X-ray Background Tool, which calculates count rates from the ROSAT All-Sky Survey, corrected for the WRXR field of view ($3.25° \times 3.25°$). The count rate measurements were then converted in the HEASARC WebPIMMS tool to obtain an integrated soft X-ray flux (ergs/cm^2/s) over the applicable

energy range. A model spectrum of Vela was created in XSPEC using an absorbed equilibrium plasma model (phabs*apec) based on a best-fit model from Lu & Aschenbach,[14] with column density NH = 0.018×10^{22} cm^{-2} and temperature kT = 0.17 keV, at solar elemental abundances. The emission measure in XSPEC was scaled to force the integrated flux of the model in the given energy band to match the output from WebPIMMS. The simulated spectrum is shown in Fig. 2. Based on the model spectrum, the WRXR spectrometer was designed to maximize throughput in two orders of OVII while also capturing a single order of OVIII and CVI.

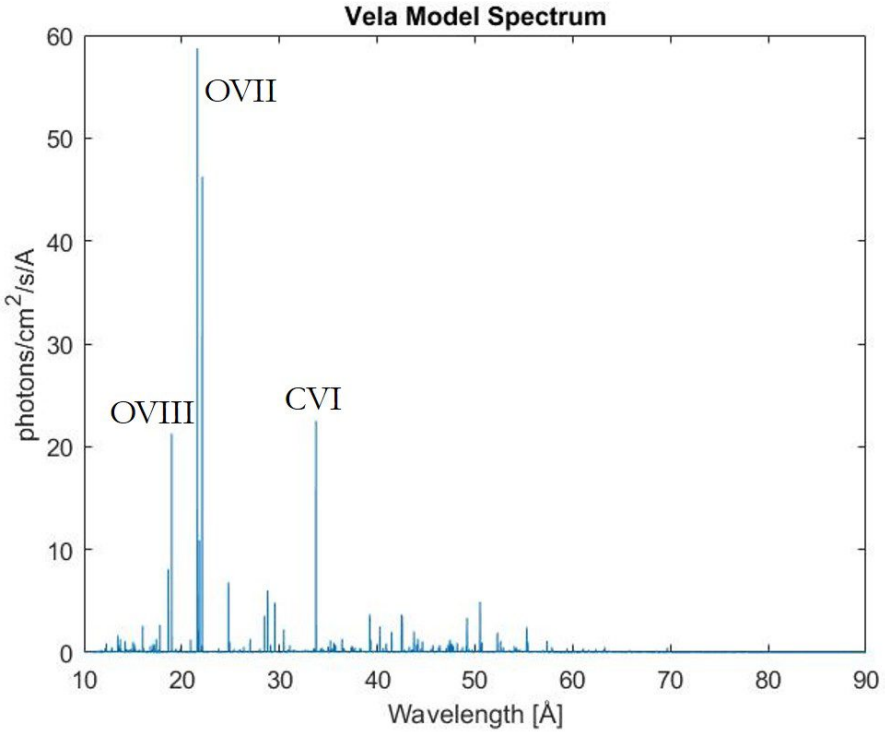

Figure 2. A simulated spectrum of the Vela supernova remnant. OVII is expected to be the dominant emission line, with contributions from CVI and OVIII also anticipated.

3. DIFFUSE SOFT X-RAY SPECTROMETER DESIGN

The WRXR spectrometer will enable a technology demonstration in a space environment for two instrument components that have been identified by the NASA Physics of the Cosmos Program as key technologies for the future of X-ray astronomy:[15] X-ray reflection gratings (Sec. 3.2) and hybrid CMOS detectors (Sec. 3.3).[16] A mechanical collimator and mirror array complete the primary components of the spectrometer, which has a 2-meter focal length and $3.25° \times 3.25°$ field of view.

3.1 Mechanical collimator

As an alternative to traditional grazing-incidence X-ray focusing mirrors, which offer high resolution at the expense of mass and cost, the WRXR spectrometer utilizes a lightweight, inexpensive collimating optic that sacrifices resolving power but achieves a large field of view. Though the mechanical collimator offers no spatial resolution, it does enable large-scale observations and information can be gathered on macroscopic conditions in diffuse sources. The collimator, schematically shown in Fig. 3, is composed of a series of 24 wire-grid plates, each 100 × 100 mm with 185 slits that sample adjacent sections of the sky. The slit widths in the collimator plates converge over ∼0.9 m from 0.724 mm to 0.500 mm so that a sculpted beam is formed naturally from the incident light; the collimator does not actively focus the light, but instead blocks any incident light that does not

match the natural convergence of the collimating slits. The resulting beam is converging in one dimension and unconstrained in the others. Due to the convergence angle, each slit samples a portion of the sky that overlaps with the adjacent slits so that each differential element of the sky in the 3.25° field of view in the direction of convergence is sampled an average of ∼4.4 times, yielding ∼14.3° of effective sky sampling in the 1D convergence direction.

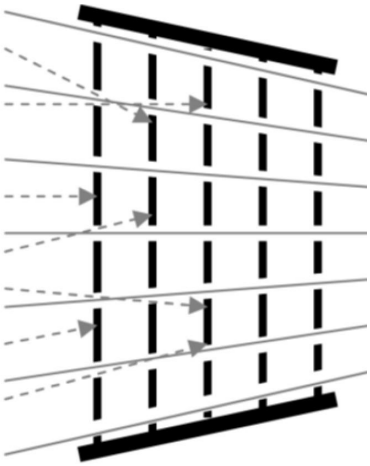

Figure 3. A schematic representation of the WRXR collimator.[1] The slits (not shown to scale) converge over 0.9 m and block any incident light that does not match the instrument's convergence.

3.2 X-ray reflection gratings and mirrors

Before the light from the collimators is allowed to reach the focal plane, an array of X-ray gratings intercepts the incident light and disperses the radiation into a spectrum of its constituent components. The gratings used in the WRXR spectrometer are off-plane reflection gratings developed as part of a study for X-ray gratings to be used on future X-ray observatories. The gratings are designed, fabricated and aligned at Penn State University.

Compared to traditional in-plane gratings, off-plane gratings are rotated ∼90° about the grating normal, which places the grating facets approximately parallel to the incident light as shown in Fig. 4. The light is then diffracted in a conical pattern according to the off-plane grating equation,[17]

$$sin\alpha + sin\beta = \frac{n\lambda}{dsin\gamma}\,, \tag{1}$$

where γ is the half-cone opening angle between the incident beam and the groove direction, d is the groove spacing, λ is the wavelength of the diffracted light, n is the order number, α represents the azimuthal angle of the reflected light along a cone with half-angle γ, and β is the azimuthal angle of the diffracted light. The gratings in Fig.4b show the Littrow configuration, an orientation in which $\alpha = \beta = \delta$, the grating groove facet angle. In this configuration, specular reflection (called 0 order in the figure) is offset azimuthally by an angle α, and light is preferentially diffracted to a specific order placed at azimuth angle β in order to maximize throughput for a particular wavelength.

The gratings in the WRXR spectrometer were designed to maximize throughput at the 3rd and 4th order emission lines of OVII, which is expected to be the dominant source of emission in the field of view. In order to achieve high throughput in the lines of interest, the gratings were blazed to an angle of 29.5° and have a variable groove spacing averaging 5750 grooves/mm. Each grating is then yawed about the grating normal to an angle of 1.25° to achieve the Littrow configuration. Light is incident on each grating at a graze angle of 2.2°, set to maximize the combination of diffraction efficiency (which is proportional to the reflectivity of the material, a quantity dependent on graze angle) and geometric throughput. Each grating in the array has a physical size of 100 × 110 mm, where the 110 mm dimension is in the cross-dispersion direction and is determined by the size of

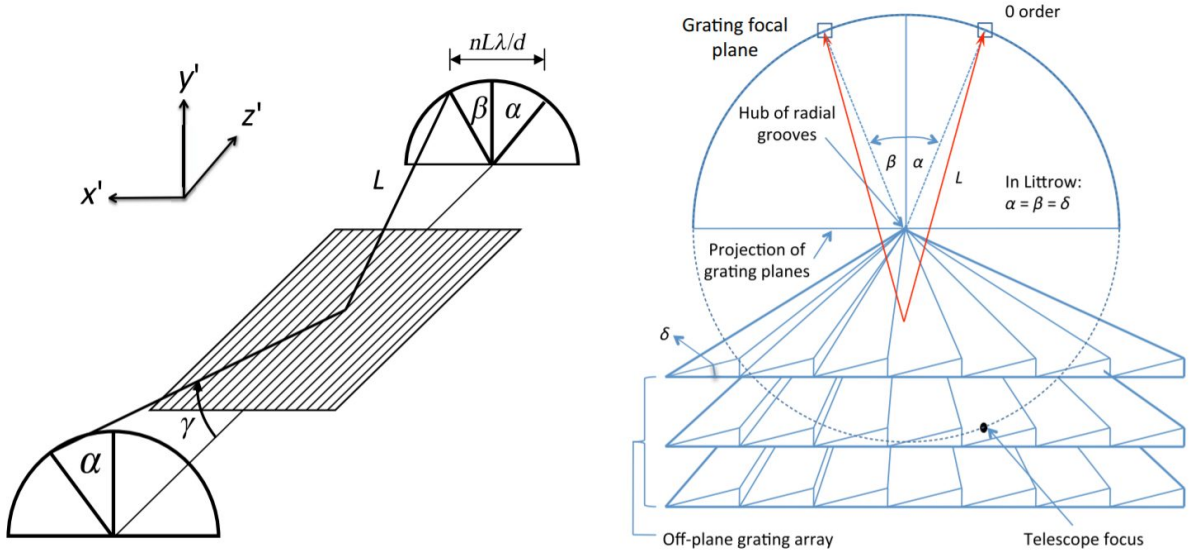

Figure 4. Diffraction geometry of off-plane gratings.[17] (a) At left, light incident quasi-parallel to the groove direction is diffracted into an arc at the focal plane according to Equation 1. The distance L is known as the throw and represents the distance from the grating to the position of the diffracted light on the focal plane. (b) At right, three co-aligned gratings intercept the light that would converge at the focal plane and instead diffract the light onto an arc. In reality, the gratings are separated from the focal plane by several meters, but the image projects the gratings to the focal plane to demonstrate the shared hub and radial convergence. These gratings are placed in the Littrow configuration so that light is preferentially diffracted at the position indicated by the angle β.

the collimator beam at the position of the grating array, and the 100 mm dimension is set to allow the maximum effective area from a 150 mm wafer (the wafer size on which the gratings are written). In order to maximize reflectivity (and therefore diffraction efficiency), the gratings are coated with 15 nm of Ni. Ni was chosen for the WRXR gratings because of its consistently high reflectivity of X-rays in the energy range $\sim$0.25 – 0.80 keV, the bandpass in which the Vela supernova remnant emits soft X-rays.

In addition to the diffraction efficiency, which drives the graze angle, blaze angle, and groove density of the gratings, the spectral resolving power of the gratings must be considered. To minimize any grating-induced aberrations to the line spread function (LSF), the grating grooves should have a radial profile in which each individual groove converges to the same point at the focal plane. However, the energy resolution of the WRXR spectrometer is primarily limited by the collimator, which produces an LSF that is $\sim$1.80 mm. For an LSF of this size, an approximation to a radial profile can be made without a significant loss in resolving power; an analysis of the spectrometer design indicated that approximating a radial profile with segments of parallel gratings widens the WRXR LSF by less than 5% compared to a true radial groove pattern. As a result, the gratings in the WRXR spectrometer were designed to have five 20-mm long sections of parallel grooves that approximate a radial pattern and are considerably simpler to fabricate.

The primary line of interest for this flight, the OVII triplet, has an energy of $\sim$570 eV, corresponding to a wavelength of $\sim$2.17 nm. Using an equation for grating dispersion,

$$x = \frac{\lambda n L}{d}\,, \tag{2}$$

where λ is the wavelength, n is the order number, L is the throw, and d is the spacing of the grating grooves, the physical displacement at the focal plane, x, of a given spectral line can be calculated.. The spectral resolving power, $x/\delta x$, can then be determined from the dispersion and the LSF. The resolving power for the WRXR spectrometer for OVII is $\sim$38 in 3rd order and $\sim$50 in 4th order.

The collimated beam of light dispersed by each individual grating is ∼80 mm at the focal plane in the cross-dispersion direction. The 26 gratings in the WRXR spectrometer grating array span a physical distance of ∼110 mm, which produces spectral lines at the focal plane that are ∼190 mm in cross-dispersion extent. The detector has an active area of 35 × 35 mm, which results in less than 20% of a given spectral line being incident on the detector. One strategy to decrease the cross-dispersion extent of the spectral lines at the focal plane is to co-align each grating so that the hub of each grating points to the same position at the focal plane as shown in Fig. 4b. However, this technique requires that the nominal graze angle of each grating vary from 2.2° for the grating at the center of the array to 2.2° ± ∼0.8° for gratings at the edges of the array. The ∼0.8° variation in nominal graze angle, coupled with the range of angles with which photons strike the grating after passing through the collimator (which causes the light to converge in only one dimension), causes a significant decrease to overall diffraction efficiency. Therefore, in order to minimize the losses from variable grazes and maximize the number of photons that fall on the detector, the gratings are all aligned to the nominal 2.2° graze angle and an array of nickel-coated mirrors are installed after the grating module to reflect the light that would fall outside of the 35 mm detector area onto the detector. The nominal graze angle of each mirror varies based on the desired displacement of the beam at the focal plane; mirrors that reflect light from gratings near the edge of the grating array have a larger graze angle in order to shift the spectral line by a larger distance at the focal plane. The beam shape and constraints on mirror alignment disallow a complete recovery of the light that falls outside the detector area. However, the mirror module will conservatively allow a factor of ∼1.5 more photons to be collected than the variable-graze method described previously. A schematic diagram of the light path through the collimator, grating array and mirror array is shown in Fig. 5, and the grating and mirror specifications are shown in Table 1.

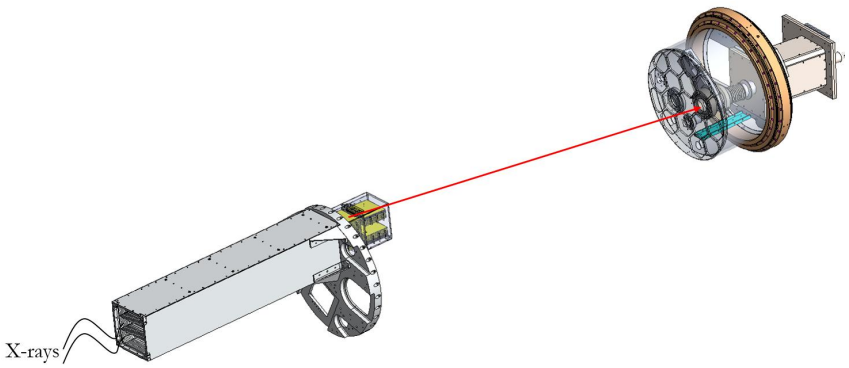

Figure 5. A schematic diagram of the WRXR spectrometer. X-rays are incident from image left and pass through the mechanical collimator before being diffracted and reflected by the grating array and mirror array, respectively. After dispersing over ∼2 m, the spectrum is imaged by the detector.

3.3 Hybrid CMOS detector and support systems

The detector used in the WRXR spectrometer is an X-ray hybrid CMOS detector (HCD) manufactured by Teledyne Imaging Sensors.[18,19] When incident on the HCD, a photon first encounters an Al filter that blocks optical light while allowing X-rays to pass through with high efficiency. The filter is followed by a Si absorber that converts X-ray photons to electrons via the photoelectric effect. The electrons are then transferred to an in-pixel CMOS readout integrated circuit that functions as a charge-to-voltage converter and initial signal processor. The absorber and readout circuit are aligned and connected together at each of the detector's 1024 × 1024 pixels by indium interconnects as shown in Fig. 6. Separating the photoelectric absorber from the pixel readout allows each component to be independently optimized to maximize the detection sensitivity and chip

Table 1. Specifications for the WRXR gratings and mirrors.

	Gratings	**Mirrors**
Quantity	26	23
Reflective Coating	Nickel	Nickel
Size	110 × 100 × 0.5 mm	110 × 100 × 0.5 mm
Nominal Graze Angle	2.2°	0.35° – 0.80°
Blaze Angle	29.5°	–
Yaw Angle	1.25°	–
Groove Density	5750 grooves/mm	–

functionality, respectively.

The HCD used in the WRXR spectrometer has 36 μm pixels and is driven by a Teledyne application-specific integrated circuit (the SIDECAR^{TM}ASIC[20]), which provides driving voltages and performs analog-to-digital conversion. A custom-built board interacts with the ASIC, provides filtered power, and handles data flow. The detector and ASIC are housed into a 6" × 6" housing that is mounted at the spectrometer's focal plane. The detector housing will be isolated from the vacuum section of the payload by a controllable gate valve, which protects the camera from external factors and provides a sub-vacuum section for the camera itself. An on-board GN2 bottle will actuate the gate valve when the instrument is pointed at Vela to enable science observation. An Fe-55 button source, which produces X-rays through radioactive decay, will be mounted on the gate valve; when the gate valve is closed, isolating the HCD from the external environment, Mg-K X-rays will be incident on the detector and will provide an in-flight calibration source. To ensure optimal operating conditions for the HCD, an on-board ion pump and LN2 cold finger will maintain vacuum pressure in the detector housing and ensure the sensor is cooled to ∼130K, respectively.

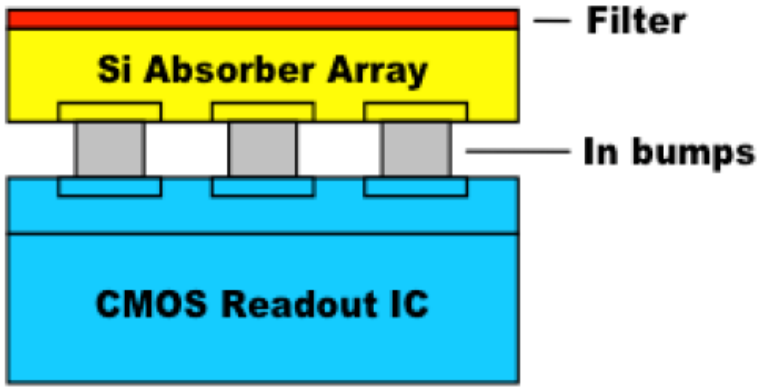

Figure 6. A diagram of the HCD. An aluminum filter allows X-rays to pass while blocking unwanted light at other wavelengths. The Si absorber array converts photons to electrons and passes the charge through In bumps to a readout integrated circuit.

4. SUMMARY

The WRXR sounding rocket payload will launch from the Kwajalein Atoll in April 2018 and will seek to be the first NASA astrophysics payload to be recovered from water. WRXR will target a 3.25° × 3.25° region in the northern part of the Vela supernova remnant and will obtain a spectrum with resolving power of ∼25-50 in the

0.25 – 0.8 keV bandpass, with the primary source of emission being OVII at 0.57 keV. The spectrometer utilizes a wire-grid collimator, X-ray reflection gratings, grazing-incidence mirrors, and a hybrid CMOS detector to perform science on a supernova remnant while developing technology for future missions. Through its combination of science, X-ray technology development, and water recovery, WRXR will offer three unique contributions to the astronomy community.

ACKNOWLEDGMENTS

The WRXR payload is funded through NASA grants NNX17AD87G and NNX15AC42G.

REFERENCES

[1] Zeiger, B.R., "Soft x-ray spectroscopy of the Vela supernova remnant," Doctoral Thesis, University of Colorado (2013).
[2] Rogers, T., McEntaffer, R., Schultz, T., Zeiger, B., Oakley, P., and Cash, W., "The OGRESS sounding rocket payload," Proc. SPIE 885911 (2013).
[3] $https://www.nasa.gov/mission_pages/sounding-rockets/overview/sites.html$
[4] Cha, A.N., Sembach, K.R., and Danks, A.C., "The Distance to the Vela Supernova Remnant," The Astrophysics Journal, 515:L25-L28 (1999).
[5] McEntaffer, R.L., and Bransteg, T., "Chandra imaging and spectroscopy of the eastern XA region of the Cygnus Loop supernova remnant," The Astrophysics Journal, 730, 99, 11 pages (2011).
[6] McEntaffer, R.L., and Cash, W., "Soft x-ray spectroscopy of the Cygnus Loop supernova remnant," The Astrophsyics Journal, 680, 328, 8 pages (2008).
[7] Seward, F.D., et al., "X-rays from Puppis A and the vicinity of Vela X," The Astrophysics Journal, 169:515-524 (1971).
[8] Gorenstein, P., Harnden, F.R., and Tucker, W.H., "The x-ray spectra of the Vela and Puppis supernova remnants and the shock-wave model of supernova remnants," The Astrophysics Journal, 192:661-676 (1974).
[9] Burkert, W., Zimmerman, H.U., Aschenbach, B., Brauninger, H., and Williamson, F., "Soft X-ray filter spectroscopy of the supernova remnants VELA X and Puppis A," Astronomy and Astrophysics 115(1), 167-170 (1982).
[10] Kahn, Steven M., Gorenstein, P., Harnden, F.R., and Seward, F.D., "Einstein observations of the Vela supernova remnant: the spatial structure of the hot emitting gas," The Astrophysical Journal, 299:821-827 (1985).
[11] Aschenbach, B., Egger, R., and Trumper, J., "Discovery of explosion fragments outside the Vela supernova remnant shock-wave boundary," Nature, 373:587-590 (1995).
[12] Bamba, A., Yamazaki, R., and Hiraga, S., "Chandra observations of the galactic supernova remnant Vela Jr.: a new sample of thin filaments emitting synchrotron X-rays," The Astrophysics Journal, 632:294-301 (2005).
[13] Gaetz,T.J., et al., "X-ray observations of the Vela supernova remnant ejecta fragments," AIP Conference Proceedings, 1156, 236 (2009).
[14] Lu, F.J., Aschenbach, B., "Spatially resolved X-ray spectroscopy of the Vela supernova remnant," Astronomy and Astrophysics, 362, 1083-1092 (2000).
[15] NASA physics of the Cosmos Program Annual Technology Report (2016).
[16] Gaskin, J., et al., "X-ray Surveyor Mission: Concept Study," Proc. SPIE 96010J (2015).
[17] McEntaffer, R.L., et al., First results from a next-generation off-plane X-ray diffraction grating, Experimental Astronomy (2013).
[18] Prieskorn, Z., Griffith, C., Bongiorno, S.D., Falcone, A.D., and Burrows, D.N., "Characterization of Si Hybrid CMOS Detectors for use in the Soft X-ray Band," Nuclear Instruments & Methods in Physics Research, 717, 83 (2013).
[19] Falcone, A.D., Burrows, D., Bai, Y., et al., "Hybrid CMOS X-ray Detectors: The Next Generation for Focused X-ray Telescopes," Proc. SPIE 668602 (2007).
[20] Teledyne Scientific and Imaging, "SIDECAR^{TM}ASIC" $http://www.teledyne-si.com/ps-sidecar-asic.html$